Mon. Not. R. Astron. Soc. **313**, 73–86 (2000)

Optical, infrared and millimetre-wave properties of Vega-like systems – IV. Observations of a new sample of candidate Vega-like sources

Roger J. Sylvester[1]★ and Vincent Mannings[2]
[1]*Department of Physics & Astronomy, University College London, Gower Street, London WC1E 6BT*
[2]*Jet Propulsion Laboratory, California Institute of Technology, MS 169-327, 4800 Oak Grove Drive, Pasadena, CA 91109, USA*

Accepted 1999 October 21. Received 1999 October 20; in original form 1999 July 1

ABSTRACT

Photometric observations at optical and near-infrared wavelengths are presented for members of a new sample of candidate Vega-like systems, or main sequence stars with excess infrared emission due to circumstellar dust. The observations are combined with *IRAS* fluxes to define the spectral energy distributions of the sources. Most of the sources show only photospheric emission at near-IR wavelengths, indicating a lack of hot (~1000 K) dust. Mid-infrared spectra are presented for four sources from the sample. One of them, HD 150193, shows strong silicate emission, while another, HD 176363, was not detected. The spectra of two stars from our previous sample of Vega-like sources both show UIR-band emission, attributed to hydrocarbon materials. Detailed comparisons of the optical and *IRAS* positions suggest that in some cases the *IRAS* source is not physically associated with the visible star. Alternative associations are suggested for several of these sources. Fractional excess luminosities are derived from the observed spectral energy distributions. The values found are comparable to those measured previously for other Vega-like sources.

Key words: circumstellar matter – planetary systems – infrared: stars.

1 INTRODUCTION

Vega-excess, or Vega-like systems are main sequence stars that exhibit infrared emission above expected photospheric levels. The best known Vega-excess stars are α Lyr itself and β Pic. The excess flux is ascribed to thermal emission from circumstellar dust grains orbiting in a disc or ring structure (see e.g. Aumann et al. 1984). Imaging of the dust emission at infrared and submillimetre wavelengths (e.g. Holland et al. 1998; Koerner et al. 1998) and coronagraphic imaging of scattered light (e.g. Smith & Terrile 1984; Schneider et al. 1999) have confirmed that the dust is indeed distributed in discs.

Many searches of the *IRAS* catalogues have found other candidate Vega-like stars (e.g. Aumann 1985; Sadakane & Nishida 1986; Walker & Wolstencroft 1988; Stencel & Backman 1991). The *Infrared Space Obsevatory* (*ISO*) has also been used to search for new Vega-likes. One notable result was the discovery of dust emission from ρ^1 Cnc (Dominik et al. 1998), a G8V star which is known to host at least one planet (Butler et al. 1997). Comprehensive reviews of the Vega-excess phenomenon and its relation to the formation of planets can be found in Backman & Paresce (1993), Ferlet & Vidal-Madjar (1994) and Lagrange, Backman & Artymowicz (2000).

★ E-mail: rjs@star.ucl.ac.uk

1.1 The new catalogue

Mannings & Barlow (1998; henceforth MB) have recently published the results of a new search for candidate Vega-like systems. The search made use of the *IRAS* Faint Source Survey Catalogue (FSC; see Moshir et al. 1992 for details). The FSC has a sensitivity limit approximately one magnitude fainter than the Point Source Catalog (PSC), achieved by co-adding the individual detector data before extracting sources. The increased sensitivity is gained at the expense of a slight reduction in the reliability of the detections (94 per cent, compared with 99.997 per cent for the PSC).

The FSC was searched for main-sequence stars by extracting sources that were positionally associated with luminosity class V stars from the published volumes of the Michigan Catalog of Two-Dimensional Spectral Types for the HD Stars (Houk & Cowley 1975; Houk 1978; Houk 1982; Houk & Smith-Moore 1988). Volumes 1–4 of the Michigan catalogue give spectral types and luminosity classes for some 130397 HD stars south of a declination $\delta = -12°$.

Cross-correlating these catalogues gave a total of 294 luminosity class V stars that have good detections in the *IRAS* bands 1–3, 1 and 2, or 2 and 3 (bands 1, 2, 3 and 4 have wavelengths of 12, 25, 60 and 100 μm respectively). Of these, 131 stars were found to show significant IR excess emission. See MB for details of the selection process.

MB searched for excess IR emission on the basis of ratios of the *IRAS* fluxes, reasoning that a fall-off of flux with wavelength that was shallower than that expected from a stellar photosphere implies excess emission. They therefore did not need to determine the expected (i.e. photospheric) fluxes in the *IRAS* bands. While this approach provides a robust method for identifying sources with excess emission, detailed analysis of the emitting material requires knowledge of the photospheric contribution to the IR fluxes.

We have therefore made optical and near-IR photometric observations of a number of the MB sources, in order to characterize their spectral energy distributions (SEDs) at wavelengths where thermal dust emission will be negligible, which allows the photospheric contribution to the SED to be calculated for all wavelengths (typically by using a model atmosphere) and to find the wavelength at which the onset of excess emission occurs. The latter is important for deriving the total excess luminosity, and the maximum temperature of the emitting dust.

2 OBSERVATIONS

26 stars from the MB sample were selected for observing on the basis of their RA and such photometry as was available in the literature. These target stars are listed in Table 1. All the new photometric observations presented here were made in 1995 September, using the facilities of the South African Astronomical Observatory. Spectra in the 10 μm band were obtained at UKIRT in 1996 September and 1998 July.

2.1 Optical photometry

Photometry was obtained in both the broad-band $UBV(RI)_C$ system and in the intermediate-band Strömgren *uvby* system. Both sets of observations were made using the Modular Photometer on the 0.5-m reflector at the SAAO Sutherland site. See Kilkenny et al. (1998) and Kilkenny & Laing (1992) for details of the use of this instrument, the adopted standard star systems and the data reduction procedures for $UBV(RI)_C$ and *uvby* photometry respectively.

An aperture of 25 arcsec was used, and sky background measurements were made for each star that was observed. The data were reduced by SAAO staff, using the photometric reduction procedures described in the latter two references.

Table 1. Log of the photometric observations.

HD	SAO	HR	Other	Sp. T	*UBV*	*uvby*	nIR
7151	215402			F6V	√	√	√
10800	258271	512	GJ 67.1	G1/2V		√	
16157	215947		CC Eri	M0Vp	√	√	√
17848	248656	852	ν Hor	A2V		√	√
21563	248797	1053		A3/5V +G0/5		√	√
28001	233498			A4V	√	√	√
38905	217529			F6/7V		√	
39944	171003			G1V		√	
131885	183025			A0V			√
137751	–			F6V	√		√
139450	206837			G0/1V	√		√
145263	184196			FOV			√
150193	184536		MWC863	A1V	√	√	
153968	253795			F0V	√		√
165088	–			F5V	√		
176638	229461	7188	ζ CrA	B9/AOV		√	√
178253	210990	7254	α CrA	A0/1V			√
181296	246055	7329	η Tel	A0V			√
181327	246056			F5/6V	√	√	√
184800	246196			A8/9V	√	√	√
191089	188955			F5V	√	√	√
195627	254823	7848	ϕ^1 Pav	F0V	√	√	√
203608	254999	8181	γ Pav	F7V	√		√
214953	231257	8635	GJ 817A	G0V	√	√	√

2.2 Near-infrared photometry

Near-IR (*JHKL*) observations were made with the MkII Infrared Photometer at the Cassegrain focus of the 0.75-m reflector at Sutherland. The MkII photometer uses an InSb detector cooled by pumped liquid nitrogen, and is of similar design to the MkI instrument described by Glass (1973). Background subtraction is achieved using a sector-wheel chopper in the instrument, with a chopping frequency of 12.5 Hz. The photometer integration time was 10 seconds at a single pointing. The telescope was nodded in declination every 20 s to allow for gradients in the sky emission. An observing 'module' consists of two nodded pairs of integrations (on-off-off-on), and therefore lasts 40 seconds. For each target, sufficient modules were taken to attain an adequate signal-to-noise ratio in the co-added result.

2.3 *Hipparcos*/Tycho photometry

As well as a wealth of parallax and astrometric data, the *Hipparcos* mission (ESA 1997) produced a great deal of useful photometric data, for the pre-selected stars in the *Hipparcos* Input Catalogue, and also for more than a million stars brighter than $V \sim 11.5$ (forming the Tycho Catalogue). Stars in the *Hipparcos* catalogue have photometry in the *B*, *V* and *I* bands, derived from satellite and selected ground-based measurements, while the Tycho catalogue gives *B* and *V* magnitudes. Data from the *Hipparcos* and Tycho catalogues were used to supplement the new ground-based photometry and to check our results.

2.4 Mid-IR spectroscopy

Mid-IR spectra were taken on 1998 July 1 of four sources from the MB catalogue: HD 109085, 123356, 150193 and 176363. The data were obtained at UKIRT, using the common-user helium-cooled spectrometer CGS3 in its low-resolution ($R \approx 55$) 10 μm mode. A detailed description of CGS3 can be found in Cohen & Davies (1995). The spectra were flux calibrated by dividing the spectrum of the target by that of a standard star, then multiplying by a model of the mid-IR spectrum of the standard. α Boo was used to calibrate the HD 109085 spectrum; the model for this standard was the absolutely-calibrated spectrum of Cohen et al. (1995). HD 123356 and HD 150193 were calibrated using σ Lib, assumed to radiate as a 3640 K blackbody with a 10.0-μm flux of 188.6 Jy, while HD 176363 was calibrated using η Sgr, treated as a 3600 K blackbody with a 10.0-μm flux of 208.7 Jy.

Many of the stars in the MB list are too far south to be observed from UKIRT, so we have not attempted a comprehensive CGS3 survey. Similarly, we do not have SAAO photometry for two of the stars observed with CGS3 due to the different constraints on the two observing runs. The four MB stars observed with CGS3 were selected on criteria including their declination, *IRAS* 12-μm flux and compatibility with the scheduling of other targets on the observing night.

We also present CGS3 spectra of two stars from Sylvester et al. (1996; henceforth Paper 1), HD 34700 (SAO 112630) and HD 34282 (SAO 131926). HD 34700 is of spectral type G0V and shows strong excess emission in the *IRAS* bands, but does not show a strong near-IR excess. The A0 star HD 34282 shows excess emission at both *IRAS* and near-IR wavelengths. Radiative-transfer models of these two objects were presented by Sylvester & Skinner (1996) and Sylvester, Skinner & Barlow (1997). HD 34282 was imaged recently at $\lambda = 2.6$ mm using the Owens Valley Radio Observatory mm-wave interferometer (Mannings & Sargent 2000). The image shows an unresolved continuum source centred on the star, with an upper limit to radius of 270 au. The mass of grains is estimated to be $\sim 10^{-4}\,M_{\odot}$. Greaves, Mannings and Holland (1999) used the JCMT to measure a double-peaked CO($3 \rightarrow 2$) spectrum that can be fit with a model spectrum generated by emission from gas moving in Keplerian orbits within a disc.

The CGS3 spectra of these two objects were obtained for us as UKIRT Service observations on 1996 September 26. α Aur, assumed to radiate as a 4880-K blackbody, was used as the standard star for these observations. The adopted 10.0-μm flux for α Aur was 228.8 Jy

3 RESULTS

3.1 Photometry

The individual measurements of the $UBV(RI)_C$, *uvby* and *JHKL* magnitudes are presented in Tables 2, 3 and 4 respectively. The final adopted values, including *Hipparcos* and literature data are presented in Table 5. Of the two nights when *uvby* observations were made, it was found that the conditions on September 14th were less suitable for photometry than on the 18th, as evidenced by higher atmospheric extinction and greater residuals in the standard star observations. Wherever possible, therefore, *uvby* observations from the 14th have been discarded in favour of magnitudes obtained on the 18th, or from the literature. For the other two photometric systems, Table 5 gives the mean values for stars that were observed on more than one occasion. Carter (1990) has published accurate near-IR photometry of HD 203608 and HD 214953; our results agree reasonably well with these published values.

We can judge the reliability of our data by comparing our *V* magnitudes with *Hipparcos* and Tycho data. We find that typical discrepancies between the two data sets are 0.02 mag, which is consistent with the night-to-night differences in our observed *V* magnitudes in Table 2. Larger discrepancies were found for HD 7151 (0.24 mag) HD 16157 (0.15 mag) and HD 165088 (0.09 mag).

HD 16157 (CC Eri) is a flare star and spectroscopic binary. It shows variability at optical wavelengths with amplitudes of 0.3 mag and a period of 1.5 d (Kholopov et al. 1998). Our *V*-band

Table 2. Photometry in the $UBV(RI)_C$ system.

HD	Date	*U*	*B*	*V*	*R*	*I*
7151	Sep 12	10.368	10.356	9.946	9.713	9.481
	Sep 13	10.404	10.385	9.967	9.727	9.487
16157	Sep 12	11.245	10.133	8.758	7.869	6.941
	Sep 15	11.200	10.089	8.724	7.835	6.925
28001	Sep 16	9.994	9.943	9.728	9.614	9.498
137751	Sep 13	9.869	9.840	9.316	9.033	8.724
139450	Sep 13	9.369	9.339	8.773	8.454	8.128
150193	Sep 12	9.697	9.376	8.821	8.424	7.953
	Sep 17	9.678	9.375	8.823	8.435	7.939
153968	Sep 17	9.841	9.666	9.315	9.096	8.833
165088	Sep 12	10.109	10.140	9.674	9.387	9.086
181327	Sep 12	7.490	7.504	7.032	6.769	6.501
	Sep 13	7.503	7.516	7.043	6.772	6.513
184800	Sep 12	10.158	10.055	9.765	9.601	9.449
191089	Sep 13	7.579	7.626	7.169	6.902	6.646
195627	Sep 13	5.094	5.031	4.751	4.578	4.411
203608	Sep 13	4.608	4.710	4.219	3.924	3.613
214953	Sep 13	6.599	6.536	5.978	5.654	5.333

Table 3. Photometry in the Strömgren *uvby* system.

HD	Date	*y*	$b-y$	m_1	c_1
7151	Sep 14	9.938	0.264	0.167	0.568
	Sep 18	9.981	0.268	0.166	0.545
10800	Sep 14	6.015	0.427	0.182	0.297
	Sep 18	5.898	0.403	0.162	0.307
16157	Sep 14	8.801	0.882	0.516	0.051
	Sep 18	8.752	0.896	0.513	0.004
17848	Sep 14	5.292	0.064	0.182	1.005
	Sep 18	5.250	0.055	0.188	1.000
21563	Sep 18	6.139	0.310	0.177	0.811
28001	Sep 14	9.806	0.118	0.205	0.863
	Sep 18	9.772	0.140	0.175	0.855
38905	Sep 18	9.757	0.342	0.172	0.360
39944	Sep 18	9.537	0.367	0.158	0.329
150193	Sep 14	8.944	0.401	0.060	1.016
176638	Sep 14	4.755	−0.001	0.139	1.016
181327	Sep 18	7.037	0.304	0.165	0.419
184800	Sep 18	9.774	0.172	0.190	0.809
191089	Sep 14	7.168	0.300	0.156	0.405
	Sep 18	7.181	0.300	0.165	0.397
195627	Sep 14	4.752	0.190	0.184	0.728
214953	Sep 14	5.968	0.356	0.182	0.367
	Sep 18	5.982	0.362	0.176	0.372

Table 4. Individual *JHKL* measurements. Figures in parentheses are statistical errors in millimag.

HD	Date	*J*	*H*	*K*	*L*
7151	Sep 5	9.129(97)	8.926(70)	8.783(62)	
	Sep 11	8.751(13)	8.413(11)	8.366(7)	8.320(666)
16157	Sep 9	5.852(9)	5.099(4)	4.901(12)	4.865(21)
17848	Sep 5	5.079(8)	5.045(4)	5.025(5)	4.982(18)
	Sep 11	5.091(3)	5.036(3)	5.023(3)	5.010(15)
21563	Sep 9	5.096(10)	4.697(6)	4.594(12)	4.598(28)
	Sep 11	5.051(3)	4.636(3)	4.574(3)	4.530(15)
28001	Sep 10	9.362(20)	9.194(18)	9.230(32)	
38905	Sep 11	8.875(16)	8.580(5)	8.538(5)	
131885	Sep 11	6.184(3)	6.737(3)	6.722(7)	6.936(137)
137751	Sep 10	8.361(10)	8.090(9)	8.046(15)	
139450	Sep 10	7.755(8)	7.438(8)	7.399(7)	7.313(212)
145263	Sep 9	8.153(9)	7.932(7)	7.884(14)	7.397(268)
153968	Sep 11	8.350(8)	8.301(9)	8.249(13)	8.554(798)
176638	Sep 5	4.768(8)	4.769(4)	4.780(5)	4.738(26)
178253	Sep 5	4.007(8)	3.981(4)	3.973(5)	3.944(17)
181296	Sep 5	5.019(8)	5.022(4)	5.025(5)	5.001(24)
	Sep 11	5.020(3)	5.022(3)	5.025(3)	5.026(31)
181327	Sep 9	6.197(8)	5.978(4)	5.932(12)	5.852(33)
	Sep 11	6.215(3)	5.979(3)	5.940(4)	5.951(53)
184800	Sep 9	9.220(20)	9.090(22)	9.099(28)	
	Sep 11	9.250(10)	9.124(24)	9.036(29)	
191089	Sep 5	6.355(8)	6.118(4)	6.093(7)	6.095(146)
	Sep 10	6.346(8)	6.122(3)	6.092(5)	6.013(58)
195627	Sep 9	4.223(9)	4.085(4)	4.039(12)	4.012(19)
203608	Sep 9	3.263(9)	2.952(4)	2.900(12)	2.886(15)
214953	Sep 5	4.921(8)	4.592(4)	4.537(5)	4.465(15)
	Sep 9	4.927(8)	4.593(4)	4.515(12)	4.552(15)
	Sep 11	4.929(3)	4.569(3)	4.531(3)	4.490(18)

Table 5. Combined optical and near-IR photometry.

HD	*U*	*B*	*V*	*R*	*I*	Ref	*y*	$b-y$	m_1	c_1	Ref	*J*	*H*	*K*	*L*	Ref
7151	10.39	10.37	9.96	9.72	9.48		9.981	0.268	0.166	0.545		8.90	8.67	8.57	8.32	
10800	6.58	6.48	5.87		5.22	(1,2)	5.898	0.403	0.162	0.307		4.86	4.53	4.48	4.40	(3)
16157	11.22	10.10	8.74	7.85	6.93		8.752	0.896	0.513	0.004		5.85	5.10	4.90	4.87	
17848		5.35	5.25		5.14	(2)	5.250	0.055	0.188	1.000		5.09	5.04	5.02	5.00	
21563	6.88	6.63	6.15		5.59	(1,2)	6.139	0.310	0.177	0.811		5.06	4.65	4.58	4.54	
28001	9.99	9.94	9.73	9.61	9.50		9.772	0.140	0.175	0.855		9.36	9.19	9.23		
38905		10.28	9.72			(2)	9.757	0.342	0.172	0.360		8.88	8.58	8.54		
39944		10.12	9.58			(2)	9.537	0.367	0.158	0.329						
109 085	4.71	4.69	4.32	3.94	3.76	(1)		0.244	0.167	0.543	(5)	3.69	3.57	3.54	3.51	(4)
123356		10.77	10.11			(2)										
131885		6.93	6.91		6.88	(2)						6.81	6.74	6.72		
137751	9.87	9.84	9.32	9.03	8.72							8.36	8.09	8.05		
139450	9.37	9.34	8.77	8.45	8.13			0.371	0.150	0.328	(5)	7.76	7.44	7.40	7.31	
145263		9.43	8.97		8.44	(2)						8.15	7.93	7.88	7.4	
150193	9.69	9.38	8.82	8.43	7.95		8.944	0.401	0.060	1.016		7.06	6.32	5.51	4.19	(6)
153968	9.84	9.67	9.32	9.10	8.83			0.226	0.154	0.895	(5)	8.53	8.30	8.25	8.6	
165088	10.11	10.14	9.67	9.39	9.09											
176363		9.98	9.78			(2)										
176638	4.66	4.73	4.75		4.76	(1,2)	4.755	-0.001	0.139	1.016		4.77	4.77	4.78	4.74	
178253	4.24	4.15	4.11	4.07	4.07	(1)		0.018	0.184	1.060	(5)	4.08	3.98	3.97	3.94	
181296		5.05	5.03		4.99	(2)		0.000	0.157	1.002	(5)	5.02	5.02	5.03	5.02	
181327	7.50	7.51	7.04	6.77	6.51		7.037	0.304	0.165	0.419		6.21	5.98	5.94	5.90	
184800	10.16	10.06	9.77	9.60	7.45		9.774	0.172	0.190	0.809		9.23	9.11	9.07		
191089	7.58	7.62	7.17	6.90	9.45		7.181	0.300	0.165	0.397		6.35	6.12	6.09	6.08	
195627	5.09	5.03	4.75	4.58	4.41		4.752	0.190	0.184	0.728		4.22	4.09	4.04	4.01	
203608	4.61	4.71	4.22	3.92	3.61			0.331	0.124	0.313	(5)	3.26	2.95	2.90	2.98	
214953	6.60	6.54	5.98	5.65	5.33		5.982	0.362	0.176	0.372		4.93	4.59	4.53	4.50	

References for observations in the literature: (1) Johnson 1966, (2) *Hipparcos* and Tycho Catalogues, (3) Engels et al. 1981, (4) Paper I, (5) Hauck & Mermilliod 1998, (6) Hillenbrand et al. 1992.

observations and the Tycho *V* magnitude lie within the normal range of variations. Whitelock et al. (1991) have monitored the star in the near-IR and have found variations with amplitude 0.2 mag at *J*. Again, our new data are consistent with the observed range of values. Tsikoudi (1988) showed that the *IRAS* PSC fluxes at 12 and 25 μm are consistent with photospheric emission. The PSC gives only upper limits for the 60- and 100-μm fluxes of this source, but the FSC gives detections in both of these bands, with fluxes significantly in excess of the expected photospheric values. We therefore retain the object in our sample, with the caveat that it is far from being a 'normal' Vega-like star.

HD 7151 is flagged in the Tycho catalogue as a suspected variable on the basis of the photometric measurements. Kukarkin et al. (1982) also list it as a suspected variable, with *V* in the range 9.40–9.48, which is significantly brighter than both the Tycho measurements and our own *UBV* and Strömgren observations. It therefore appears possible that the amplitude of the long-term variability of this star is significantly greater than the range given by Kukarkin et al. Our near-IR photometry shows significant differences (e.g. $\Delta J = 0.38$) between the two observing nights; this is probably also due to intrinsic variability.

On the other hand, the Tycho catalogue gives no indication of variability for HD 165088, nor have we found any reports of variability in the literature. For this source, the discrepancy between our observations and the Tycho magnitudes may therefore be due to observational error.

Strömgren photometry for several stars in our sample is available in the catalogue of Hauck & Mermilliod (1998). Agreement between our observations and these published magnitudes is good. For the eight stars in Table 3 which are included in Hauck & Mermilliod, typical discrepancies are <0.01 mag. We can therefore conclude that our photometric data are certainly of sufficient quality for our primary purpose, i.e. defining optical and near-IR SEDs.

3.2 Spectral energy distributions

The optical and near-IR photometry can now be combined with the colour-corrected *IRAS* fluxes in order to construct optical-IR SEDs for all our sources. This allows us to determine the excess flux at all four *IRAS* wavelengths. As the MB selection criteria required only knowledge of the gradient of a source's SED, they did not determine the size of the excess at any given wavelength.

As in Paper 1, we converted magnitudes in the *UBVRI* and *JHKL* systems to absolute flux densities using the flux calibration of Deacon (1991) and Cohen et al. (1992). For the Strömgren data, we adopted the calibration of Lamla (1982). Where Strömgren colours were taken from the literature and no *y* magnitude was specified, we simply assumed that $y = V$. Whilst not strictly correct, due to the different widths of the *y* and *V* bands, this is sufficiently accurate for the purpose of defining an SED. For example, comparison of the *y* and *V* magnitudes in Table 5 shows that the offset between the two bands is rather small; the average value of $|V - y|$ is 0.02 mag. Similarly, the approximate formula $V = y - 0.12[(b-y) - 0.55]^2$ given by Budding (1993) shows that one can expect $V - y \approx 0.04$ mag for an early A star, with smaller differences for later spectral types. Our simplifying assumption will therefore affect the absolute fluxes in the Stromgren bands by less than 5 per cent. The reddening, $E(B-V)$, towards each star was determined from the observed $B-V$ colour and the intrinsic colours tabulated by Schmidt-Kaler (1982). The derived values of $E(B-V)$ range from -0.07 to 0.16 (see Table 6), indicating that none of our sources suffers strong interstellar or circumstellar extinction with a normal reddening

Table 6. Derived quantities. Tabulated are the reddening $E(B-V)$, the ratio of the *IRAS* 12-μm flux to the expected photospheric flux, the fractional excess luminosity and the separation (in arcsec) between the *IRAS* and optical positions. Values in parentheses indicate stars for which the association between the *IRAS* and HD objects is questionable.

HD	Sp. T	$E(B-V)$	$\frac{F_{12,\mathrm{FSC}}}{F_{12,*}}$	L_{IR}/L_*	sep
7151	F6V	−0.07	(451)	(0.29)	54
10800	G1/2V	0.00	1.4	2×10^{-4}	12
16157	M0Vp	−0.04	0.92	3×10^{-4}	1
17848	A2V	0.05	1.2	4×10^{-5}	3
21563	A3/5V	0:	1.4	8×10^{-5}	5
28001	A4V	0.14	(10.8)	(8×10^{-3})	55
38905	F6/7V	0.05	(7.2)	(6×10^{-3})	21
39944	G1V	−0.06	(6.4)	(1×10^{-2})	22
109085	F2V	0.04	1.6	3×10^{-5}	2
123356	G1V	0.05	93	5×10^{-2}	1
131885	A0V	0.02	(2.7)	(8×10^{-4})	27
137751	F6V	0.05	(76)	(8×10^{-2})	43
139450	G0/1V	−0.01	(20)	(4×10^{-2})	42
145263	FOV	0.16	23	2×10^{-2}	12
150193	A1V	0.55	346	0.37	7
153968	F0V	0.09	(27)	(2×10^{-2})	27
165088	F5V	0.03	(2006)	(1.8)	16
176363	A2V	0.15	(228)	(3×10^{-2})	59
176638	B9/AOV	0.00	1.7	2×10^{-4}	18
178253	A0/1V	0.04	1.9	6×10^{-5}	2
181296	A0V	0.04	2.1	3×10^{-5}	6
181327	F5/6V	0.00	1.7	2×10^{-3}	10
184800	A8/9V	0.04	(159)	(8×10^{-2})	68
191089	F5V	0.01	1.4	2×10^{-3}	4
195627	F0V	−0.02	1.3	1×10^{-4}	9
203608	F7V	0.00	1.6	1×10^{-5}	18
214953	G0V	−0.02	1.3	6×10^{-5}	1

law. The fluxes for stars with $E(B-V)>0.04$ were dereddened using a Galactic reddening curve based on the fits of Seaton (1979) and Howarth (1983). The apparent negative reddenings observed towards some of our targets were presumed not to have a physical origin, but to result from errors in the observed colours, the spectral types and/or in interpolating the intrinsic colours to a particular spectral subtype. Effective temperatures were derived from the *uvby* photometry using the grids of Moon & Dworetsky (1985). These temperatures were then converted into spectral classes using the Gray & Corbally (1994) calibration, allowing us to independently check the Michigan classifications for our sources. Good agreement was found between the Michigan and *uvby* classes, with discrepancies of less than one spectral subtype for most of our sources. For two of the three sources in Table 6 which have negative $E(B-V)$ values, the *uvby* spectral type (F3V for HD 7151, G0V for HD 39944) is slightly earlier than the Michigan type. Adopting these new spectral types would give small positive reddenings for both stars.

The SEDs are presented in Figs 1 and 2, along with normalized Kurucz (1991) model atmospheres with temperatures appropriate for the spectral types of the stars. HD 21563 has a composite spectral type of A3/5 + G0/5 (see Table 1). The optical SED is consistent with a 6000 K model atmosphere (i.e. spectral type G0V) and no reddening. The SED presented in Fig. 1 shows the 6000-K atmosphere and the observed fluxes with no dereddening applied. If, however, the A-type component dominates the optical emission (as would be expected if both components are main-sequence stars and lie at the same distance), then a reddening of $E(B-V)\approx0.35$ should be adopted.

The relative strength of the mid-IR dust emission was measured in terms of $F_{12,\mathrm{FSC}}/F_{12,*}$, the ratio of the *IRAS* 12-μm flux to the predicted photospheric flux, derived from the normalized model atmospheres. It is of interest to compare the SEDs obtained for the MB catalogue with those derived in Paper 1, in order to see if the two sets of objects have similar disc and stellar properties. All six of the Paper 1 stars with $(F_{12,\mathrm{FSC}}/F_{12,*})\geqslant20$ show clear excess emission at *H*, *K* and *L*. In the new sample, there are ten stars with similarly large $F_{12,\mathrm{FSC}}/F_{12,*}$ values. We have near-IR photometry for seven of these stars, and only one of them, HD 150193, shows strong near-IR excess like the Paper 1 stars (HD 145263 appears to show a small excess at *L*, but the error on this measurement is rather large).

There does, therefore, appear to be a significant difference between the dust emission properties of the two groups of stars. The apparent sudden onset of dust emission, from being negligible at *L*, to more than an order of magnitude greater than the photosphere at 12 μm, is very remarkable (but see below).

3.3 Positional associations

The strong excess in the *IRAS* bands for stars with no near-IR excess made it worthwhile to re-examine some of the associations between *IRAS* sources and HD stars proposed by MB.

We searched the Tycho astrometric results to obtain accurate optical co-ordinates for our stars and computed the separation between the optical and *IRAS* FSC positions. The results are given in Table 6. The proper motions of the sources in the ∼8-year interval between the *IRAS* and *Hipparcos* missions were taken into account when determining the separations. The ratio $F_{12,\mathrm{FSC}}/F_{12,*}$ is plotted against these separations in Fig. 3. Inspection of Fig. 3 reveals that most of the sources with substantial 12-μm excesses have large separations (≳20 arcsec) between the *IRAS* and optical positions. By contrast, for most of the stars with $F_{12,\mathrm{FSC}}/F_{12,*}\sim1$, i.e. where the *IRAS* flux is dominated by photospheric emission, the optical and *IRAS* sources coincide to within 10 arcsec. If the IR flux from all our sources was truly circumstellar emission, one would expect that the typical separation for stars with large excesses would be the same as for stars with small excesses. The major axis of the FSC positional uncertainty ellipse is typically 10–20 arcsec for our sources, consistent with the separations of the low-excess sources, but smaller than those of the high-excess sources. It therefore appears that the MB associations between the optical and *IRAS* sources for source separations ≳20 arcsec are questionable.

Searching the Tycho catalogue showed that the *IRAS* FSC source associated by MB with HD 7151 lies nearer to the M2 star CPD-43 142. Fitting a 2500-K blackbody to the Tycho *V* magnitude of this star gave good agreement to the *IRAS* data. We therefore conclude that CPD-43 142, not HD 7151, is the true IR source. In all other cases, the Tycho data showed no star nearer to the *IRAS* position than the HD star listed by MB.

We investigated further by conducting searches of the HST Guide Star Catalog and USNO PMM astrometric catalogue, centred on the *IRAS* FSC positions. These catalogues are based on Schmidt photographic surveys, and have a fainter limiting magnitude than Tycho. We also searched the SIMBAD database and the Digital Sky Survey images to check for other possible associations. In eleven cases (see Table 7), other sources were found which lay closer to the *IRAS* position than did the HD stars associated by MB. For six of these, the alternative association seems more plausible than the MB star; this was typically because the alternative candidate lay within a few arcseconds of the *IRAS*

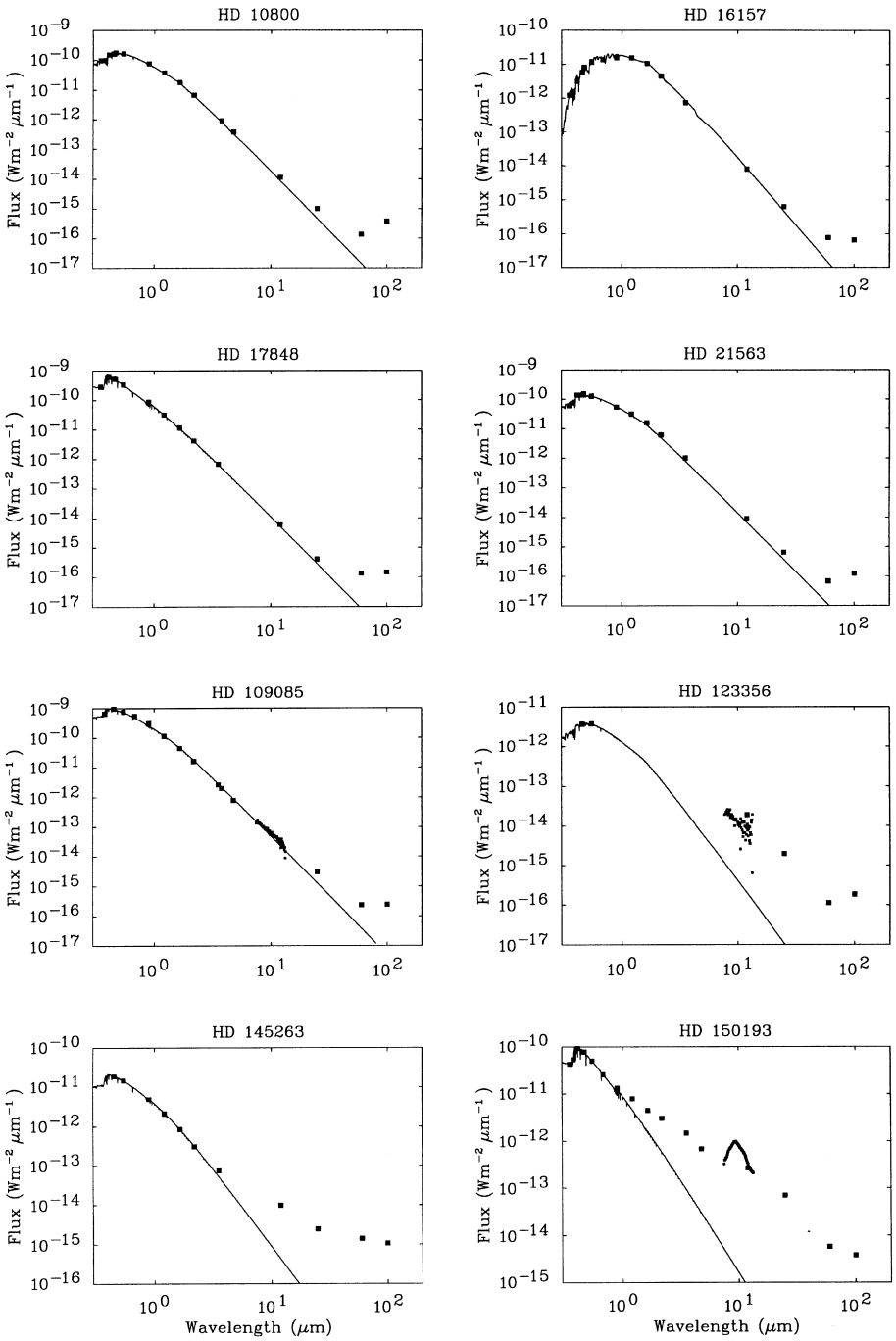

Figure 1. Spectral energy distributions for the sources with separations between optical and *IRAS* positions of less than 20 arcsec. Larger filled squares: ground-based, *Hipparcos* and *IRAS* photometry; smaller filled squares: CGS3 spectra; lines: model atmospheres.

position and was likely to be bright in the IR. For the remaining five objects, it is more difficult to determine whether the alternative optical source is the true counterpart of the *IRAS* source: ESO 488−41 and GSC08401−00331 are not very close to the *IRAS* position, while GSC09039−00816 is faint but not red ($B \approx 11.1$, $R \approx 11.4$), and so is likely to be even fainter than HD 153968 at 12 μm. USNO 0450−02210000 and 0600−17362689 are very faint ($R \approx 18$ and 17 respectively) and are also not too close to the *IRAS* position.

In the other 16 cases, the MB star was the most likely optical counterpart to the *IRAS* source. These objects are generally the sources with low 12-μm excess fluxes and small separations between the *IRAS* and optical positions.

Several of the 'alternative' associations are cool stars: CPD-43 142 has spectral type M2, IK Lup is an M0 T Tauri star, V2090 Sgr is a Mira variable, and GSC07839−00442 and GSC08401−00331 have approximate $B-R$ colours (from the USNO catalogue) of 3.7 and 1.9 respectively. *IRAS* 18027−4455 was found by te Lintel Hekkert et al. (1991) to show double-peaked OH maser emission at 1612 MHz, and so is presumably an optically-faint OH/IR star. Two of the other potential counterparts are galaxies: NGC 1574 and ESO 488−41.

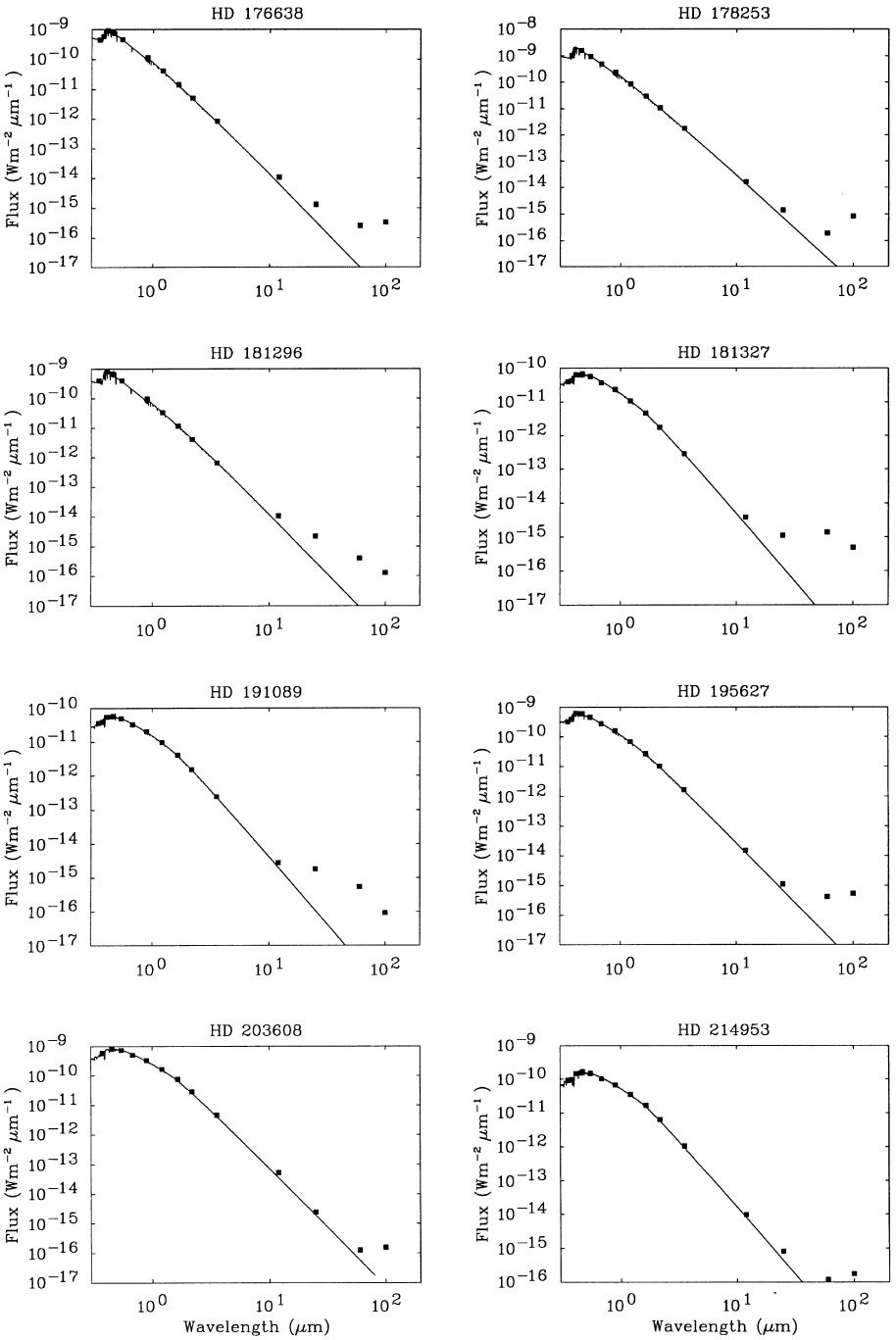

Figure 1 – *continued*

Mid-IR imaging with better spatial resolution than *IRAS* would make it possible to unambiguously determine whether the IR source is associated with the optical star in these cases. As demonstrated in section 3.4, ground-based mid-IR spectroscopy (with small apertures) is also able to verify positional associations. The new near-infrared surveys (e.g. 2MASS, DENIS) will also be useful in this regard.

3.4 Mid-IR spectra

The new CGS3 spectra are presented in Fig. 4, while SEDs including the CGS3 data for the four MB stars are included in Fig. 1. The observations of the six sources give rather varied results: emission with a strong silicate feature (HD 150193), weak excess emission (HD 123356), a basically photospheric spectrum (HD 109085), a complete non-detection (HD 176363) and UIR (unidentified infrared) bands from the two Paper I sources.

Fig. 4 also shows the *IRAS* 12-μm FSC fluxes, which have been colour-corrected using the shapes (but not the absolute fluxes) of the CGS3 spectra. Agreement between *IRAS* and CGS3 is good for HD 109085 and HD 150193, while for the other two sources, the CGS3 spectrum lies significantly below the *IRAS* point. The difference in flux is approximately 1 Jy for HD 123356 and 1.3 Jy for HD 176363. The expected photospheric emission from the

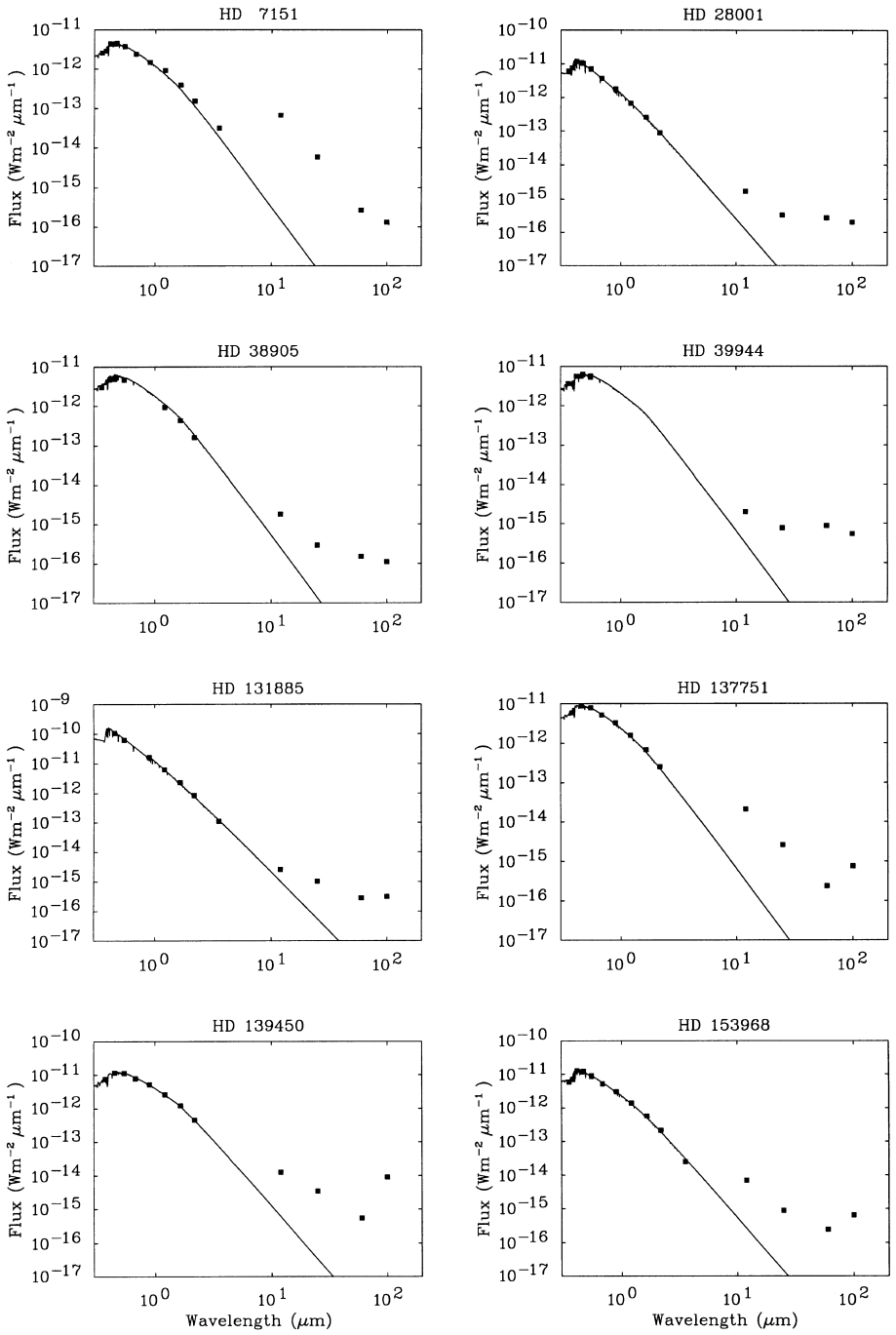

Figure 2. Spectral energy distributions for the sources where the optical and *IRAS* positions are separated by more than 20 arcsec. Filled squares: ground-based, *Hipparcos* and *IRAS* photometry; small open squares: 3-σ upper limits derived from CGS3 data (see text); lines: model atmospheres.

stars, derived from fitting Kurucz model atmospheres to the optical photometry, is also plotted in Fig. 4

Only in the case of the optically bright, nearby star HD 109085 ($V = 4.3$, 18 pc) is the photosphere bright enough in the IR to be detected by CGS3 with the modest integration times that we used. In fact, we find that 75–90 per cent of the observed flux over the whole observed wavelength range can be attributed to photospheric emission. The excess spectrum, after subtracting the model atmosphere, is approximately constant at $F_\lambda \approx 1.2 \times 10^{-14}\,\mathrm{W m^{-2} \mu m^{-1}\,W}$ shortwards of 11 μm, then tends towards zero for the remainder of the spectrum. The CGS3 spectrum and the *IRAS* photometry are consistent with weak excess emission arising from material at temperatures of a few hundred K. Such emission would give a fractional excess luminosity L_{IR}/L_* of approximately 4×10^{-4}.

It is clear that although our observed flux for HD 123356 lies significantly below the *IRAS* measurement, we still detect substantial excess emission from this source. The ratio of observed to photospheric flux at 10.0 μm is approximately 27. The *IRAS* 12-μm flux was measured with a beam substantially larger than the 5.5-arcsec aperture employed with CGS3, so it is possible that the IR emission is extended, and roughly half of the total flux

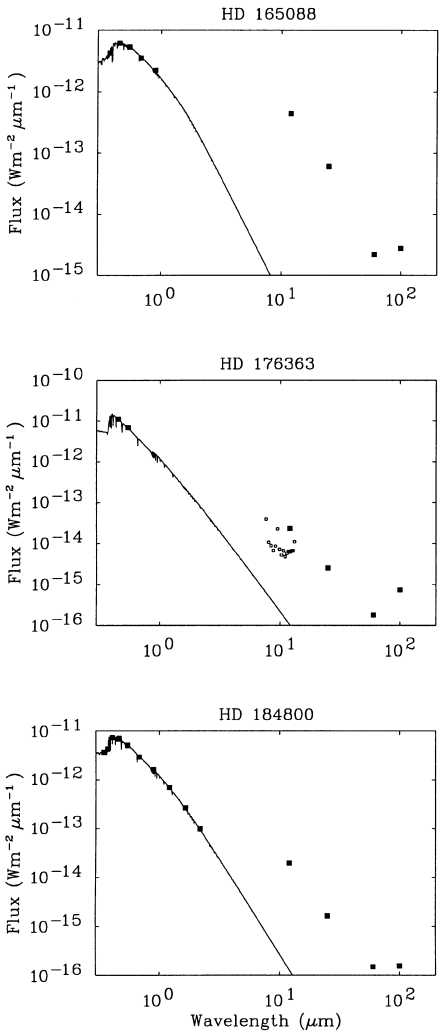

Figure 2 – *continued*

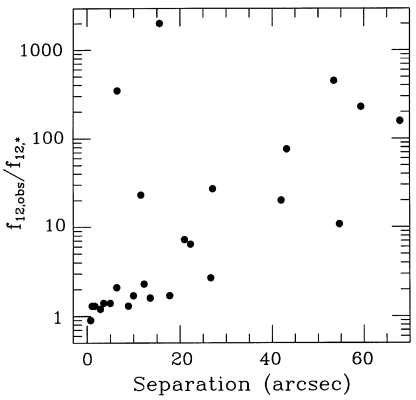

Figure 3. Ratio of observed to stellar 12-μm flux plotted against the separation between the the *IRAS* and optical positions.

Table 7. Details of the MB stars for which other possible associations for the *IRAS* sources were found. Upper group: Sources where the 'alternative' association is more plausible than the HD star; lower group: sources with ambiguous data. See text for details. Columns headed 'sep' are the separation in arcsec between the *IRAS* FSC position and the HD star or other object.

FSC Source	MB Association HD	sep	Other Association Source	sep
01089–4257	7151	54	CPD-43 142	18
04210–5705	28001	55	NGC1574	10
15258–3956	137751	43	GSC07 839–00442	2
15362–3436	139450	42	IK Lup	2
18027–4455	165088	16	OH/IR star	–
18578–2138	176363	59	V2090 Sgr	3
05455–4054	38905	21	USNO0450–02210000	10
05526–2535	39944	22	ESO 488–41	14
14539–2605	131885	27	USNO0600–17362689	16
17019–6004	153968	27	GSC09 039–00816	5
19347–5106	184800	68	GSC08 401–00331	15

arises from outside the CGS3 beam. HD 123356 is listed in the Washington double star catalogue as having a companion separated by 2.5 arcsec, and some 2.2 mag fainter in *V*. Pointing at the primary star would therefore put the secondary close to the edge of the 5.5-arcsec diameter beam of CGS3. If a substantial portion of the IR emission arises from the secondary star, CGS3 might not have detected all of the flux. The spectrum shows a continuum decreasing with wavelength, and no evidence of silicate or SiC in emission or absorption, or of the UIR bands. The steep increase to longer wavelengths beyond 13 μm is probably spurious, due to imperfect cancellation of atmospheric absorption.

The spectrum of HD 150193 shows a very strong silicate emission feature, peaking at 9.3 μm, somewhat short of the canonical peak wavelength of 9.7 μm. This feature rises above strong excess continuum emission (see Fig. 1). Even at 7.5 μm, where the silicate feature is weak and the photospheric emission is relatively strong, the observed flux is some 65 times stronger than the expected continuum flux. As well as appearing in the MB catalogue, HD 150193 is classed as a Herbig Ae star by Finkenzeller & Mundt (1984). Inspection of its SED shows it to have a much stronger excess than most of the other stars in the present sample. In fact, both the 10-μm spectrum and the SED are similar to those of HD 144432 (SAO 184124; Paper 1), another star which has been listed as a Vega-like source and as a Herbig Ae/Be star.

Some substructure is visible in the spectrum, appearing as inflections or weak emission bands at 8.2 and 11.3 μm superposed on the silicate feature. Peaks at the latter wavelength can be due to either crystalline silicates or the hydrocarbon carriers of the UIR bands. Both UIR and crystalline silicate bands have been observed in Herbig Ae/Be stars, for example in the *ISO* SWS spectrum of HD 100546 (Malfait et al. 1998). No other UIR bands appear to be present in the HD 150193 spectrum, and the 3.3-μm UIR band is not seen around this source (Brooke, Tokunaga & Strom 1993), so the observed 11.2-μm emission feature is more likely to be due to crystalline silicates than to UIR bands. Finding candidates for the possible 8.2-μm feature is more problematic. The standard suite of UIR bands has peaks at 7.7 and 8.7 μm, neither of which match closely with the observed peak. Likewise, crystalline silicates do not show features near the observed wavelength (see e.g. Koike, Shibai & Tuchiyama 1993).

Hanner, Brooke & Tokunaga (1995) have also obtained a 10-μm spectrum of HD 150193, and discussed the possible presence of an 11.2-μm feature, which we can now confirm to be real. Their spectrum also shows a dip near 9.8 μm, but they were unable to determine its reality, due to the significant telluric ozone absorption in that wavelength region. Our spectrum shows no such

structure, so we can conclude that the feature considered by Hanner et al. is indeed spurious. Examination of the Hanner et al. spectrum suggests that an inflection at around 8.3 μm, similar to the apparent feature in our data, may also be present.

Our observations of HD 176363 failed to detect any IR flux at all. Even after re-binning the spectrum by a factor of 4 to increase the signal-to-noise ratio, the observations are consistent with zero flux (note that the photospheric flux at 10 μm, ∼7 mJy, is indistinguishable from zero for these observations). Fig. 2 plots the 3-σ upper limits derived after re-binning; they are clearly inconsistent with the *IRAS* 12-μm point. During the observations, the (optical) star was visible in the UKIRT guiding/acquisition monitor, and the coordinates that were used agree well with the positions given in the Tycho catalogue. We can therefore be sure that CGS3 was indeed observing HD 176363.

However, as shown in Section 3.3, the *IRAS* source is more likely to be associated with the Mira variable V2090 Sgr than with the HD star. We obtained a CGS3 spectrum of V2090 Sgr on the same night as the observations of the MB stars; the V2090 Sgr spectrum shows silicate emission, with a 12-μm flux level consistent with that of the *IRAS* source. We can therefore confirm that the *IRAS* source is associated with V2090, rather than with HD 176363.

The spectra of the two Paper 1 stars, HD 34282 and HD 34700, are rather noisy because of the faintness of the sources and the limited integration times available. However, in both sources we have detected emission in the UIR bands at 11.3 and 7.7 μm. HD 34282 also shows the 8.6-μm band, on the wing of the stronger 7.7-μm feature. All these bands are ascribed to hydrocarbon materials, such as polycyclic aromatic hydrocarbons. The 7.7 and 11-μm bands have been observed in a number of Vega-excess stars, while the 3.3-μm UIR band has been detected in two such sources (Paper 1, Coulson & Walther 1995, Sylvester et al. 1997). The bands are seen in the spectra of Herbig Ae/Be stars, and in a few T Tauri stars (Hanner, Brooke & Tokunaga 1995, 1998). Natta & Krügel (1995) have modelled emission from PAHs around young stars, and find that although late-type stars (such as T Tauri stars and HD 34700) are predicted to emit in the UIR bands, the features are not usually observed because they are swamped by strong continuum emission from the star or disc.

HD 34282 and HD 142666, another Paper 1 star, both show photometric variations indicative of variable obscuration by circumstellar dust in an edge-on disc (Bogaert & Waelkens 1991; Meeus, Waelkens & Malfait 1998). As noted by Sylvester et al. (1997), the distances to HD 34282 derived from the *Hipparcos* parallax (163^{+67}_{-37} pc) and from the dereddened photometry (547 pc) are inconsistent; this could be explained by the presence of an additional 2.6 mag of (grey) extinction in the disc. According to Meeus et al. HD 144432 is likely to be oriented nearly pole-on to us. The CGS3 spectra of these three sources are significantly

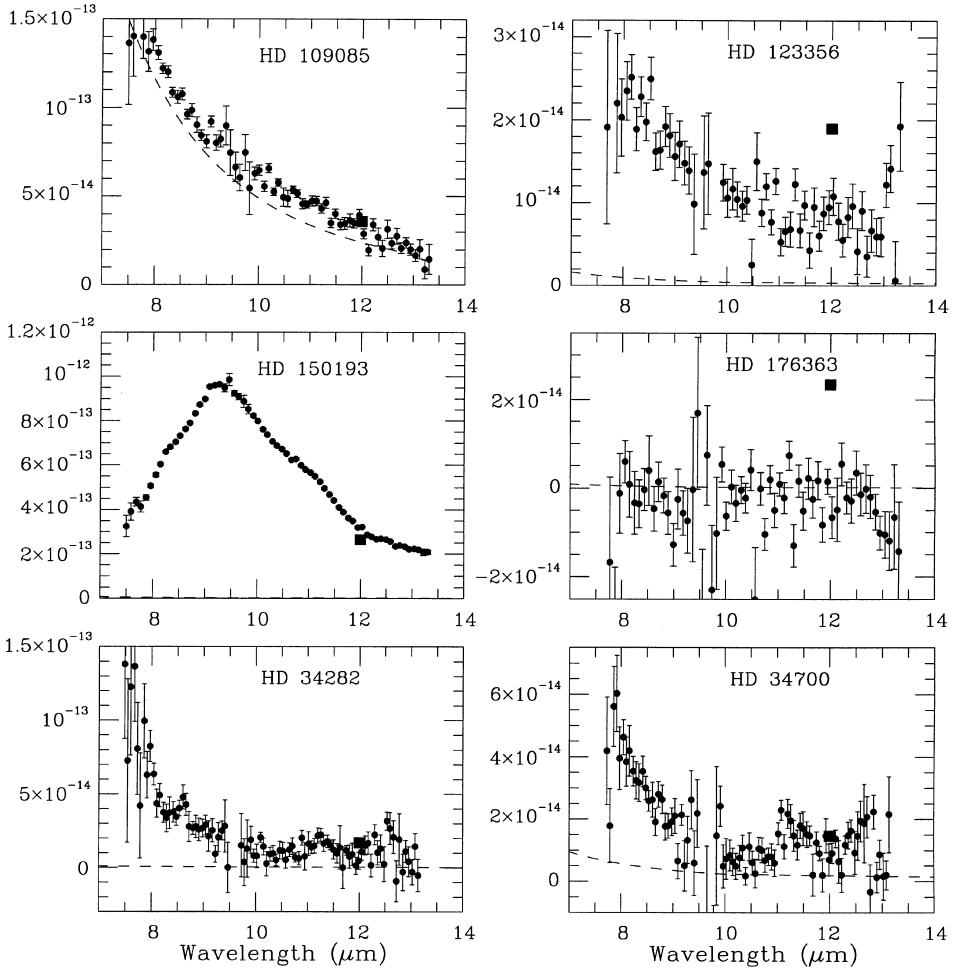

Figure 4. CGS3 spectra of four sources from the MB catalogue. Filled circles with errorbars: CGS3 spectra; large filled squares: 12-μm *IRAS* fluxes; dashed lines: predicted photospheric spectra.

different (see Fig. 4 and Paper 1): HD 144432 shows a very strong silicate feature, while HD 142666 shows UIR bands and a weaker silicate feature and HD 34282 appears to show only the UIR bands. It is tempting to see this range of features as a sequence of increasing suppression of the silicate feature with inclination angle, and hence optical depth along the line of sight; however, detailed optically-thick modelling of a large sample of Vega-like and Herbig Ae/Be stars is required to disentangle the effects of disc physical properties (grain composition, temperature structure etc) and optical depth on the observed spectra.

3.5 Hertzsprung–Russell diagram

The *Hipparcos* parallax measurements allow us to determine the distance and hence the luminosity of a number of our sources (see Table 8). To do this we derived the bolometric flux density (corrected for IS/CS extinction) by integrating under the Kurucz model atmospheres which had been normalized to the dereddened photometry. The luminosity can then simply be obtained by multiplying by $4\pi d^2$ where d is the distance. This is very similar to the method used by van den Ancker et al (1997) for their work on Herbig Ae/Be stars. The wavelength coverage of the Kurucz model atmospheres obviously does not extend to infinity, but the portion of the stellar SED beyond the longest wavelength included in the models (typically 80 μm) makes a negligible contribution to the luminosity ($\sim 10^{-6}$ of the total).

Having calculated the luminosities, we can put our sources on an H–R diagram, adopting the Gray & Corbally (1994) calibration of $T_{\rm eff}$ versus spectral type (see Fig. 5). For most of our objects, the error in the parallax makes the dominant contribution to the luminosity uncertainty. Other sources of uncertainty, such as error in the photometry, the dereddening and fitting the model atmospheres, only become important for stars closer than a few tens of pc, where the parallax is well measured. Typical errors in $\log(T_{\rm eff})$ are $\sim$0.02.

Also displayed in Fig. 5 are the Palla & Stahler (1993) evolutionary tracks for stars of mass 0.6, 0.8, 1.0, 1.5, 2.0 and 2.5 $M_\odot$. These tracks end at the ZAMS; inspection of the diagram suggests that most of our stars are either on or near the main sequence. This is to be expected, given that the MB sample is intended to include only stars with Michigan main-sequence classifications. However, accurate determination of the evolutionary state of our targets is difficult, as stars move slowly in the HR diagram in the later stages of their pre-MS evolution. For example, HD 150193, known to be a Herbig Ae star, occupies a position in Fig. 5 close to those of other A-type stars in our sample which are not thought to be Herbig Ae stars.

4 DISCUSSION

We have calculated the fractional excess luminosity, $L_{\rm IR}/L_*$, for each of our sources, by integrating the observed SEDs and the normalized model atmospheres (see Paper I for details of the method employed). $L_{\rm IR}/L_*$ is a measure of the fraction of starlight which is absorbed and re-emitted by circumstellar dust, and hence indicates the optical depth of the disc. The derived values (Table 6) are rather sensitive to assumptions about the wavelength at which excess emission becomes significant: this gives rise to an uncertainty of about a factor 2 in $L_{\rm IR}/L_*$. Measurements for stars for which the association with the *IRAS* source is suspect are included for completeness, and are shown in parentheses. The

Table 8. *Hipparcos*-based results and data used to construct the H-R diagram. Values in parentheses indicate stars for which the optical–*IRAS* association is questionable.

HD	HIP	π	Dist	$\log T_{\rm eff}$	$\log L_*/L_\odot$
10800	7601	36.9 ± 0.5	$27.1^{+0.4}_{-0.3}$	3.76	$0.41^{+0.01}_{-0.01}$
16157	11964	86.9 ± 0.9	$11.51^{+0.11}_{-0.11}$	3.59	$-1.03^{+0.02}_{-0.02}$
17848	13141	19.7 ± 0.5	$50.7^{+1.3}_{-1.2}$	3.95	$1.29^{+0.03}_{-0.03}$
21563	15840	5.5 ± 0.5	182^{+18}_{-15}		
109085	61174	54.9 ± 0.6	$18.2^{+0.2}_{-0.2}$	3.85	$0.70^{+0.02}_{-0.02}$
131885	73150	8.2 ± 0.9	121^{+14}_{-12}	4.00	$1.40^{+0.10}_{-0.09}$
(137751	75808	5.5 ± 1.4	180^{+60}_{-40}	3.81	$0.73^{+0.26}_{-0.20}$)
(139450	76675	13.6 ± 1.2	73^{+7}_{-6}	3.77	$0.12^{+0.08}_{-0.07}$)
145263	79288	8.6 ± 1.2	116^{+19}_{-14}	3.86	$0.61^{+0.13}_{-0.11}$
150193	81624	6.7 ± 1.7	150^{+50}_{-30}	3.98	$1.42^{+0.25}_{-0.20}$
176638	93542	17.8 ± 0.9	56^{+3}_{-3}	4.02	$1.60^{+0.05}_{-0.05}$
178253	94114	25.5 ± 0.8	$39.2^{+1.3}_{-1.2}$	3.99	$1.54^{+0.04}_{-0.04}$
181296	95261	21.0 ± 0.7	$47.7^{+1.6}_{-1.5}$	4.00	$1.32^{+0.04}_{-0.04}$
181327	95270	19.8 ± 0.8	51^{+2}_{-2}	3.81	$0.49^{+0.04}_{-0.04}$
191089	99273	18.7 ± 0.9	54^{+3}_{-2}	3.82	$0.47^{+0.05}_{-0.05}$
195627	101612	36.3 ± 0.7	$27.6^{+0.5}_{-0.5}$	3.86	$0.84^{+0.03}_{-0.03}$
203608	105858	108.5 ± 0.6	$9.22^{+0.05}_{-0.05}$	3.80	$0.13^{+0.02}_{-0.02}$
214953	112117	42.5 ± 0.7	$23.6^{+0.4}_{-0.4}$	3.77	$0.25^{+0.03}_{-0.03}$

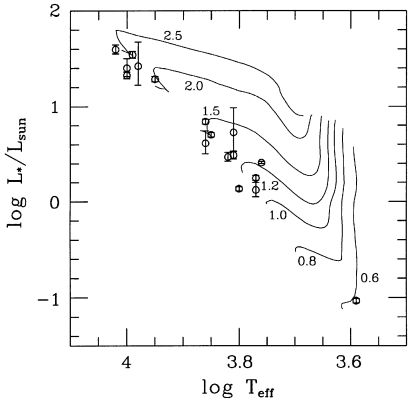

Figure 5. Hertzsprung-Russell diagram for the stars with *Hipparcos* parallaxes. Also plotted are pre-MS evolutionary tracks from Palla & Stahler (1993), which are labelled with the stellar mass ($M_\odot$).

excess fluxes in the *IRAS* wavebands for the 'bona-fide' MB candidates (i.e. those which lie within 20 arcsec of their *IRAS* counterparts) are presented in Table 9. These define the SED of the dust emission.

HD 150193 shows a large $L_{\rm IR}/L_*$, greater than the maximum value (0.25) for passive re-radiation by a physically thin disc (Kenyon & Hartmann 1987); this suggests that the disc is self-luminous due to accretion. The stars in Paper I which have been classified as Herbig Ae/Be stars have similar values of $L_{\rm IR}/L_*$. Several stars in the present sample have fractional luminosities in the range $\sim 10^{-5}$–10^{-4}, comparable with those of the prototypical Vega-excess stars α Lyr and α PsA (Gillett 1986). The stars that show excess emission at 12 μm have fractional luminosities of $\sim 10^{-3}$–10^{-2}, similar to those of the Paper I stars which do not show near-IR excess emission.

Of the 16 'bona fide' MB stars (i.e. the stars in Fig. 1), four (25 per cent) show *IRAS* 12-μm fluxes which exceed the predicted photospheric flux by more than a factor of 2. We have near-IR photometry of three stars in this group; of these, only HD 150193,

Table 9. Excess fluxes (i.e. observed-photospheric) in the *IRAS* wavebands.

HD	Excess flux (Jy)			
	12 μm	25 μm	60 μm	100 μm
10800	0.12 ± 0.04	0.12 ± 0.02	0.14 ± 0.03	1.22 ± 0.21
16157	−0.02 ± 0.03	0.03 ± 0.02	0.07 ± 0.02	0.21 ± 0.04
17848	0.03 ± 0.02	0.02 ± 0.01	0.15 ± 0.03	0.48 ± 0.10
21563	0.11 ± 0.02	0.05 ± 0.01	0.07 ± 0.01	0.40 ± 0.07
109085	0.59 ± 0.13	0.35 ± 0.06	0.23 ± 0.04	0.78 ± 0.25
123356	0.90 ± 0.09	0.40 ± 0.11	0.13 ± 0.04	0.60 ± 0.15
145263	0.43 ± 0.07	0.51 ± 0.08	1.69 ± 0.40	3.56 ± 0.80
150193	12.09 ± 0.70	14.35 ± 0.67	6.72 ± 0.44	12.1 ± 2.1
176638	0.20 ± 0.05	0.20 ± 0.04	0.29 ± 0.06	1.10 ± 0.26
178253	0.16 ± 0.06	0.15 ± 0.05	0.20 ± 0.06	2.53 ± 0.58
181296	0.23 ± 0.02	0.39 ± 0.03	0.46 ± 0.05	0.42 ± 0.08
181327	0.06 ± 0.03	0.20 ± 0.02	1.62 ± 0.07	1.65 ± 0.21
191089	0.04 ± 0.03	0.35 ± 0.05	0.65 ± 0.06	0.31 ± 0.08
195627	0.12 ± 0.06	0.09 ± 0.03	0.48 ± 0.07	1.76 ± 0.43
203608	0.89 ± 0.12	0.11 ± 0.04	0.09 ± 0.04	0.52 ± 0.10
214953	0.09 ± 0.04	0.08 ± 0.03	0.13 ± 0.04	0.56 ± 0.13

(which is a Herbig AeBe star), shows a clear excess at near-IR wavelengths. By comparison, 16 out of 23 (∼70 per cent) of the Paper 1 stars showed 12-μm excess, while 9 of them showed near-IR excess. Despite the relatively small samples, we can surmise that the incidence of excess near-IR and mid-IR emission in the present sample is much lower than for the Paper 1 (i.e. Walker & Wolstencroft) stars.

The difference between the SEDs of the stars in the two samples can be ascribed to the different selection criteria employed by Walker & Wolstencroft (1988) and MB, accentuated by the choice of MB stars included in the present sample. Walker & Wolstencroft imposed a lower limit on the 60/100-μm flux ratio for their sources. A dust distribution emitting with a low 60/100-μm ratio is likely to be dominated by cool (∼50 K) grains and so will not emit strongly in the near-IR or 12-μm bands. The MB catalogue had no lower limit on the 60/100-μm ratio, and so can be expected to include a higher proportion of stars without near-IR or 12-μm excesses. The MB approach did detect a number of stars with such excesses; however, these stars had also been detected by Walker & Wolstencroft and were investigated in Paper 1, and hence were excluded from the present sample.

The lack of near- and mid-IR excess emission implies that the stars in the new sample (excluding HD 150193) therefore have negligible amounts of hot (∼1000 K) dust. Fitting blackbodies to the 25- and 60-μm excess fluxes in Table 9 gives temperatures in the range 70–150 K for most of our targets. These blackbody fits underestimate the excess flux at both 12 and 100 μm, indicating that material at a range of temperatures is present around each star. The stars with little or no 12-μm excess, such as HD 191089 and 195627, have SEDs that resemble those of the optically bright stars in Paper 1, e.g. SAO 91022 and SAO 147886. The dust discs around these objects probably resemble those around the prototypical Vega-excess stars, more than the hotter, dustier discs of the stars with near-IR excess.

An evolutionary sequence has been proposed (e.g. Waelkens et al. 1994; Malfait, Bogaert & Waelkens 1998; Yudin et al. 1999) in which the IR excess of a star declines with time, as the discs are cleared of dust by processes such as planet formation. In this scenario, stars with strong near-IR excesses, e.g. the Walker & Wolstencroft (1988) stars, are younger than those without a near-IR excess and are closely related to the Herbig Ae/Be stars. Habing et al. (1999) determined from *ISO* observations that most stars younger than 300 Myr have discs, while most stars older than 400 Myr do not. Vega itself is ∼350 Myr old, but the time-scale for dust removal processes is ∼1 Myr, implying that its dust is being replenished, presumably by erosion of larger bodies (Aumann et al. 1984). The Habing et al. results indicate that this replenishment does not continue indefinitely, although the authors did find a few stars of age several Gyr which have retained their discs.

Many of the Walker & Wolstencroft (1988) stars with near-IR excess show optical emission lines, indicating that the stars are young (Zuckerman 1994; Dunkin, Barlow & Ryan 1997). The prototype Vega-excess stars (which show no near-IR excess) do not display this phenomenon. It is therefore likely that the majority of the new MB stars are established main-sequence stars, and are significantly older than most of the Walker & Wolstencroft objects. The optical spectra of the MB stars are thus expected to show little emission activity; high-resolution spectroscopy will be useful to verify this prediction, and hence the evolutionary scenario for Vega-like discs. The MB stars with the strongest excesses, such as HD 181327 and HD 191089, would be of particular interest, as they might be the youngest members of the sample.

ACKNOWLEDGMENTS

We wish to thank the South African Astronomical Observatory for the allocation of observing time, the SAAO staff for their assistance at the telescopes and for reducing the optical photometry, and Prof. Mike Barlow for many useful discussions. The United Kingdom Infrared Telescope is operated by the Joint Astronomy Centre on behalf of the U.K. Particle Physics and Astronomy Research Council. We are grateful to the UKIRT Service team for obtaining some of our data as part of the UKIRT Service Programme. This work made use of the Simbad database and other facilities maintained at the CDS, Strasbourg.

REFERENCES

Aumann H. H., 1985, PASP, 97, 885
Aumann H. H. et al., 1984, ApJ, 278, L23
Backman D. E., Paresce F., 1993, in Levy E. H., Lunine J. I., eds, Protostars & Planets III. Univ. of Arizona, Tucson, p. 1253
Bastian U., Roeser S., 1993, Catalogue of Positions and Proper Motions – South. Astronomisches Rechen-Institut, Heidelberg
Bogaert E., Waelkens C., 1991, in Jaschek C., Andrillat Y., eds, The infrared spectral region of stars. Cambridge University Press, Cambridge, p. 345
Brooke T. Y., Tokunaga A. T., Strom S. E., 1993, AJ, 106, 656
Budding E., 1993, An Introduction to Astronomical Photometry. Cambridge University Press, Cambridge
Butler R. P., Marcy G. W., Williams E., Hauser H., Shirts P., 1997, ApJ, 474, L115
Carter B. S., 1990, MNRAS, 242, 1
Chan S. J., Kwok S., 1988, ApJ, 334, 362
Cohen M., Davies J. K., 1995, MNRAS, 276, 715
Cohen M., Walker R. G., Barlow M. J., Deacon J. R., 1992, AJ, 104, 1650
Cohen M., Witteborn F. C., Walker R. G., Bregman J. D., Wooden D. H., 1995, AJ, 110, 275
Coulson I. M., Walther D. M., 1995, MNRAS, 274, 977
Deacon J. R., 1991, PhD thesis, University of London
Dominik C., Laureijs R. J., Jourdain de Muizon M., Habing H. J., 1998, A&A, 329, L53
Dunkin S. K., Barlow M. J., Ryan S. G., 1997, MNRAS, 290, 165

Engels D., Sherwood W. A., Wamsteker W., Schultz G. V., 1981, A&AS, 45, 5
ESA 1997, The Hipparcos and Tycho Catalogues, ESA SP-1200
Ferlet R., Vidal-Madjar A., 1994, Circumstellar Dust Disks and Planet Formation. Editions Frontières, Gif sur Yvette
Finkenzeller U., Mundt R., 1984, A&AS, 55, 109
Gillett F. C., Israel F. P., 1986, Light on Dark Matter. Reidel, Dordrecht, p. 61
Glass I. S., 1973, MNRAS, 164, 155
Gray R. O., Corbally C. J., 1994, AJ, 107, 742
Greaves J. S., Mannings V., Holland W. S., 2000, Icarus, in press
Habing H. J. et al., 1999, Nat, 401, 456
Hanner M. S., Brooke T. Y., Tokunaga A. T., 1995, ApJ, 438, 250
Hanner M. S., Brooke T. Y., Tokunaga A. T., 1998, ApJ, 502, 871
Hauck B., Mermilliod M., 1998, A&AS, 129, 431
Hillenbrand L. A., Strom S. E., Vrba F. J., Keene J., 1992, ApJ, 397, 613
Holland W. S. et al., 1998, Nat, 392, 788
Houk N., 1978, Michigan Catalogue of Two-Dimensional Spectral Types for the HD Stars, Vol. 2. Univ. Michigan, Ann Arbor
Houk N., 1982, Michigan Catalogue of Two-Dimensional Spectral Types for the HD Stars, Vol. 3. Univ. Michigan, Ann Arbor
Houk N., Cowley A. P., 1975, Michigan Catalogue of Two-Dimensional Spectral Types for the HD Stars, Vol. 1. Univ. Michigan, Ann Arbor
Houk N., Smith-Moore M., 1988, Michigan Catalogue of Two-Dimensional Spectral Types for the HD Stars, Vol. 4. Univ. Michigan, Ann Arbor
Howarth I. D., 1983, MNRAS, 203, 301
Johnson H. L., Iriarte B., Mitchell R. I., Wisniewskj W. Z., 1966, Commun. Lunar Planetary Lab., 4, 99
Kenyon S. J., Hartmann L., 1987, ApJ, 323, 714
Kholopov P. N. et al., 1998, Combined General Catalogue of Variable Stars. Nauka, Moscow
Kilkenny D., Laing J. D., 1992, MNRAS, 255, 308
Kilkenny D., van Wyk F., Roberts G., Marang F., Cooper D., 1998, MNRAS, 294, 93
Koerner D. W., Ressler M. F., Werner M. W., Backman D. F., 1998, ApJ, 503, L83
Koike C., Shibai H., Tuchiyama A., 1993, MNRAS, 264, 654
Kukarkin B. V. et al., 1982, New catalog of Suspected Variable Stars. Nauka, Moscow
Kurucz R. L., 1991, in Davis Philip A. G., Upgren A. R., Janes K. A., eds, Precision Photometry: Astrophysics of the Galaxy. L. Davis Press, Schenectady, p. 27
Lagrange A.-M., Backman D. A., Artymowicz P., 2000, in Mannings V., Boss A. P., Russell S. S., eds, Protostars and Planets IV. Univ. of Arizona Press, Tuscon, in press
Lamla F., 1982, in Schaifers K., Voigt H. H., eds, Landolt-Börnstein, Numerical Data and Functional Relationships in Sci and Technology, Group VI, Astronomy, Astrophysics and Space Research, Vol. 2b. Springer-Verlag, Berlin, p. 35
Malfait K., Bogaert E., Waelkens C., 1998, A&A, 331, 211
Malfait K., Waelkens C., Waters L. B. F. M., Vandenbussche B., Huygens E., de Graauw M. S., 1998, A&A, 332, L25
Mannings V., Barlow M. J., 1998, ApJ, 497, 330 (MB)
Mannings V., Sargent A. I., 2000, ApJ, in press
Meeus G., Waelkens C., Malfait K., 1998, A&A, 329, 131
Moon T. T., Dworetsky M. M., 1985, MNRAS, 217, 305
Moshir M. et al., 1992, Explanatory Supplement to the *IRAS* Faint Source Survey, Version 2, JPL D-10015 8/92. JPL, Pasadena
Natta A., Krügel E., 1995, A&A, 302, 849
Palla F., Stahler S. W., 1993, ApJ, 418, 414
Sadakane K., Nishida M., 1986, PASP, 98, 689
Schmidt-Kaler Th., 1982, in Schaifers K., Voigt H. H., eds, Landolt-Börnstein, Numerical Data and Functional Relationships in Sci and Technology, Group VI, Astronomy, Astrophysics and Space Research, Vol. 2b. Springer-Verlag, Berlin, p. 14
Schneider G. et al., 1999, ApJ, 513, 127
Seaton M. J., 1979, MNRAS, 187, 73P
Smith B. A., Terrile R. J., 1984, Sci, 226, 1421
Stencel R. E., Backman D. E., 1991, ApJ, 75, 905
Stephenson C. B., 1973, Publ. Warner & Swasey Obs., 1d, 1
Sylvester R. J., Skinner C. J., 1996, MNRAS, 283, 457
Sylvester R. J., Barlow M. J., Skinner C. J., Mannings V., 1996, MNRAS, 279, 915 (Paper 1)
Sylvester R. J., Skinner C. J., Barlow M. J., 1997, MNRAS, 289, 831
te Lintel Hekkert P., Caswell J. L., Habing H. J., Haynes R. F., Norris R. P., 1991, A&AS, 90, 327
Tsikoudi V., 1988, AJ, 95, 1797
Urban S. E., Corbin T. E., Wycoff G. L., Martin J. C., Jackson E. S., Zacharias M. I., Hall D. M., 1998, AJ, 115, 1212
van den Ancker M. E., Thé P. S., Tjin A Djie H., Catala C., de Winter D., Blondel P. F. C., Waters L. B. F. M., 1997, A&A, 324, L33
Waelkens C., Bogaert E., Waters l.B.F.M., 1994, in The P. S., Perez M. R., van den Heuvel E. P. J., eds, ASP Conf. Ser. Vol. 62, The Nature and Evolutionary Status of Herbig Ae/Be Stars. Astron. Soc. Pac., San Francisco, p. 405
Walker H., Wolstencroft R. D., 1988, PASP, 100, 1509
Whitelock P. A., Menzies J. W., Catchpole R. M., Feast M. W., Marang F., 1991, MNRAS, 250, 638
Whitelock P., Menzies J., Feast M., Catchpole R., Marang F., Carter B., 1995, MNRAS 276, 219
Yudin R. V., Clarke D., Smith R. A., 1999, A&A, 345, 547
Zuckerman B., Ferlet R., Vidal-Madjar A., 1994, Circumstellar Dust Disks and Planet Formation. Editions Frontières, Gif-sur-Yvette, p. 131

APPENDIX A: COMPARISON OF OPTICAL AND *IRAS* POSITIONS FOR THE MB STARS

As discussed in Section 3.3, the separation between the positions of the optical star and the *IRAS* source can be a useful criterion for assessing the reality of the associations proposed by MB. In Table A1, we present the separations for all of the MB candidates which had not been identified in previous surveys (i.e. the stars in Table 2 of MB). As for the separations in Table A1, we use the Tycho optical positions, and include proper motions back to the epoch of the *IRAS* observations. A few alternative associations, obtained from searches of the SIMBAD database and the Tycho catalogue are listed, along with the separations from the *IRAS* positions. Relevant data from Table 7 are repeated here.

HD 71397 is not listed in the SAO or PPM (Positions and Proper Motions; Bastian & Roeser 1993) catalogues. The position in the HD catalogue (given with low precision) lies within 6 arcsec of that listed for the *IRAS* source, which has been associated with the carbon star CCCS 1174 (Stephenson 1973; Chan & Kwok 1988). The Tycho catalogue and the Astrographic Catalogue (AC2000; Urban et al. 1998) both list two stars within 2 arcmin of the HD position. The nearest (TYC 6002–616–1, separation = 6 arcsec) is at the position of the *IRAS* source. Tycho photometry for this star gives $B - V = 2.3$, consistent with a carbon star, but very red for a star classified as F8 (HD) or F3V (Michigan). The next-nearest star to the HD position, TYC 6002–735–1, has a much larger separation (72 arcsec), and a $B - V$ colour of 0.51, much closer to the intrinsic colours of F stars. The V magnitudes of the two Tycho stars are similar (9.7 and 10.0 respectively) and close to that listed in the HD catalogue (9.9). There is no star corresponding to TYC 6002–735–1 in the SAO or PPM catalogues. The original (BD) co-ordinates of BD-16 2450 agree with those of this star to within 17 arcsec. Confusingly, the HD catalogue associates BD-16 2450 with HD 71397. It appears that although the HD position for HD 71397 is that of TYC 6002–616–1, the HD and Michigan spectra were obtained for TYC 6002–735–1. We conclude that HD 71397 (whichever of the two

Table A1. Separations (in arcsec) between the Tycho positions for the MB stars and the associated *IRAS* sources. Other possible associations are also listed.

HD	FSC source	sep	Other association source	sep
7151	01089–4257	54	CPD-43 142	18
17848	02479–6300	3		
21563	03238–6947	5		
28001	04210–5705	55	NGC1574	10
31925	04567–1627	9		
38206	05411–1834	3		
38385	05418–3925	3		
38905	05455–4054	21	USNO0450–02210000	10
39944	05526–2535	22	ESO 488–41	14
41742	06032–4504	26		
42137	06055–3701	15		
43954	06162–1434	29		
43955	06161–1956	29		
46171	06289–1636	39	SAO 151598	5
49336	06444–3743	12		
52140	06568–3055	33	PPM 739687	11
53143	06594–6115	1		
53376	07016–3144	22		
53833	07030–3724	83		
53842	06539–8355	5		
54096	07038–4515	47	CD-452917	20
56192	07123–4629	10		
60842	07306–7316	56	S Vol	7
61950	07364–6856	11		
66591	07596–6325	5		
67199	08021–6552	8		
71397	08243–1704	:	C* 1174	1
73390	08340–5803	4		
73752	08369–2229	9		
75416	08430–7846	4		
80459	09158–6333	2		
80950	09175–7431	5		
81515	09230–3540	56		
88955	10126–4152	7		
91375	10290–7144	5		
99046	11212–3710	42	GSC007214–00200	8
99211	11223–1724	5		
100786	11332–5026	42		
105686	12074–3425	34		
108483	12253–4957	1		
110058	12369–4855	6		
114981	13118–3823	20		
117360	13288–7718	12		
120095	13452–4155	57	ESO 325–22	2
121617	13545–4645	4		
123247	14044–4827	16		
123356	14047–2050	1		
128760	14368–4519	45	EE Lup	3
129364	14402–4049	59		
131885	14539–2605	27		
137751	15258–3956	43	GSC07839–00442	2
139365	15355–2936	8		
139450	15362–3436	42	IK Lup	2
142165	15509–2423	5		
143018	15557–2558	44		
145263	16078–2523	12		
145482	16091–2747	16		
153968	17019–6004	27	GSC09039–00816	5
165088	18027–4455	16	OH/IR star	–
166841	18126–6814	19		
172776	18401–3214	40		
176363	18578–2138	59	V2090 Sgr	3
176638	18596–4210	18		
181296	19188–5431	6		
181327	19189–5438	10		
181869	19204–4042	14		
184800	19347–5106	68	GSC08401–00331	15
191089	20060–2622	5		
200800	21049–6559	40		
203608	21223–6535	14		
206310	21435–8317	46		
212283	22208–3508	63	M8 giant	–
214953	22396–4728	1		

stars the identifier refers to) is not a Vega-like star, since the *IRAS* emission is clearly associated with the carbon star.

The *IRAS* source associated by MB with HD 212283 was found by Whitelock et al (1995) to be an M8 giant star.

As in Table 6, most of the alternative associations are red stars: SAO 151598 is of spectral type M0, S Vol and EE Lup are Miras, and PPM 739687 and CPD-45 1193 have $B - V > 1$.

In total, we find that 31 of the 73 stars in Table A1 have separations between optical and *IRAS* positions which are greater than 20 arcsec. We have found alternative possible associations for 17 of these, and for two sources with smaller separations.

This paper has been typeset from a TEX/LATEX file prepared by the author.